Probing the Behavior of Confined Water by Proton-Transfer Reactions

G. Angulo, J. A. Organero, M. A. Carranza, and A. Douhal*

Departamento de Química Física, Sección de Químicas, Facultad de Ciencias del Medio Ambiente, Universidad de Castilla−La Mancha, Avenida Carlos III, S.N., 45071 Toledo, Spain

Received: July 6, 2006; In Final Form: August 30, 2006

The picosecond dynamics of a bifunctional and H-bonding molecule, 7-hydroxyquinoline (7HQ), has been studied in a reverse micelle with increasing water content. The fluorescence kinetics has a complex behavior as the water content is changed. All reactions are irreversible, and a two-step mechanism is invoked to explain the observations. H_2O/D_2O exchange and excitation energy effects show that the second step has a higher barrier and that the corresponding reaction occurs through tunneling. The results clearly indicate two regimes of water nanopool behavior switching at $W_0 \approx 5$ (W_0 = [water]/[surfactant]). Water collective dynamics explains these observations. The lower fluidity of confined water within the reverse micelle with respect to normal bulk water alters the related H-bond network dynamics and therefore is responsible for the slower proton-transfer processes.

1. Introduction

It is of current interest to elucidate the role of water in biological functions with molecular and ultrafast resolution. Small and fast structural changes in the water network are decisive events in proton or H-atom transfer.[1] However, biological water is very different from the bulk liquid. Furthermore, biological samples are most of the time too complex for research of the underlying fundamental processes. Therefore, vesicles and micelles have been proposed for mimicking nanostructured biological environments, such as protein pockets and cell membranes.[2−4] Fluorescence probes sensitive to H-bonding and proton-transfer reactions are very often used as tools for exploring these media.[5−7] Available time-resolved technology allows gaining insight into the very fast processes suffered by the probe, up to a femtosecond (fs) time scale, after initiation of the photoevents. The study of organic dyes having functional groups and structures comparable to DNA bases or amino acids in biological-like water is obviously relevant to the efforts for a better understanding of the dynamics of biological systems.

In this work, we present studies of 7-hydroxyquinoline (7HQ)[8−11] embedded in a nanopool of water inside reverse micelles formed by sodium bis(2-ethylhexyl) sulfosuccinate (AOT) (Scheme 1). 7HQ is a bifunctional probe with groups comparable to those in many biological molecules, including DNA base units. Adding water produces monodisperse microemulsions of water nanopools inside the reverse AOT micelles, and its content can be varied up to high relative water concentrations without breaking or reshaping them. 7HQ has been the subject of many studies, and its physical properties are well established.[12−15] Photophysical studies of many compounds within micelles have been reported, revealing a complex water structure and pool-size-dependent fluorescence characteristics.[16,17] Two water regions can be distinguished: a first layer solvating the negatively charged surfactant headgroups, and in which the so-called "bound" water is found, and a core of "free" water. The former is much like crystallization water, while the latter does not behave like bulk water but has a higher viscosity, lower dielectric constant, and smaller activity, among other measured properties.[12−15] This behavior is rather similar to that of water around proteins, as already stated.[1] Therefore, the aim of this work is to show how a bifunctional compound like 7HQ probes the behavior of such an environment.

While preparing this paper, we became aware of the recently published work on the same system.[18] We report and discuss our results, and show that differences in the experimental conditions, such as excitation at selected wavelengths of the 7HQ−water absorption band, give another picture of the picosecond dynamics of this probe in the nanopool. We observed another prototropic species of the probe, and that the consequence of monitoring its photophysics in the nanopool is relevant for the discernment of water behavior in confined media. This allows us to distinguish two water regimes inside the micelle below $W_0 \approx 5$ (W_0 = [H_2O]/[AOT]), where kinetics depend strongly on the amount of water, and above $W_0 \approx 5$, where the dependence almost disappears.

2. Materials and Methods

2.1. Materials. 7-Hydroxyquinoline (7HQ) (Acros, 99%), heptane (Acros, Spectrograde), deuterium oxide (Aldrich, 99.9%), and sodium bis(2-ethylhexyl) sulfosuccinate (AOT) (Fluka, Ultra >99.0%) were used as received. The Karl Fischer test shows that the percentage of water in the heptane micelle solution is about 0.15% w/v. Therefore, without adding water the reverse micelle already has a $W_0 \approx 0.6$. Milli-Q ultrapure water was used in all experiments. Reverse micelles were prepared by dissolving 0.2 M AOT in heptane and sonicating for about 30 min. This AOT concentration is well above the operational critical micelle concentration (cmc),[15] and below the maximum for the monodispersivity criterion up to $W_0 = 20$.[19] The concentration of 7HQ was less than 5×10^{-4} M in order to guarantee less than one probe molecule per micelle. Water content was changed by adding it to the stock solution of 7HQ/AOT in appropriate amounts.

* Corresponding author. Fax: +34-925-268840. E-mail: Abderrazzak.douhal@uclm.es.

10.1021/jp064257g CCC: $33.50
Published on Web 11/04/2006

SCHEME 1: Molecular Structures of 7HQ and AOT and Schematic Representation of 7HQ/H_2O in AOT/*n*-heptane Micelle[a]

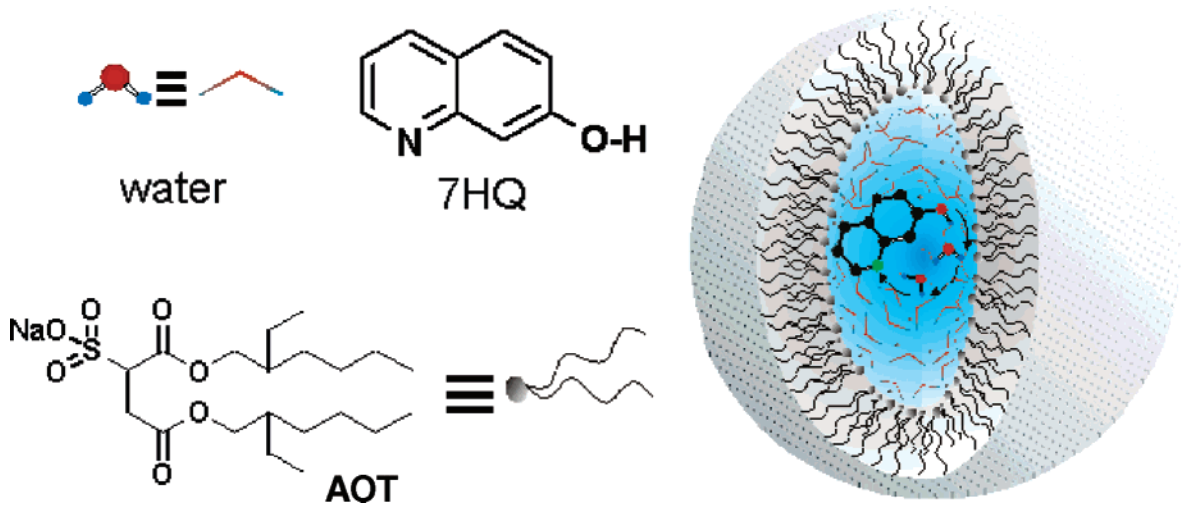

[a] For simplicity we located the probe in the center of the nanopool. The arrows indicate the proton-transfer reactions between the probe and confined water molecules.

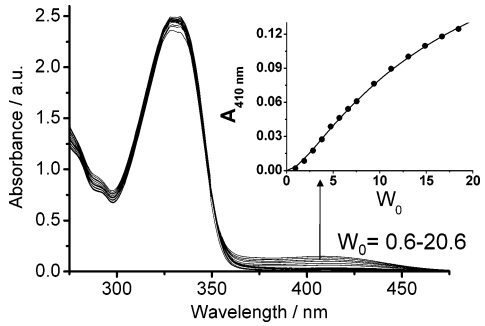

Figure 1. Absorption spectra of 7HQ in AOT/*n*-heptane reverse micelles with increasing W_0. Inset: change of absorbance at 410 nm against W_0, fitted by 1:2 complex formation model.

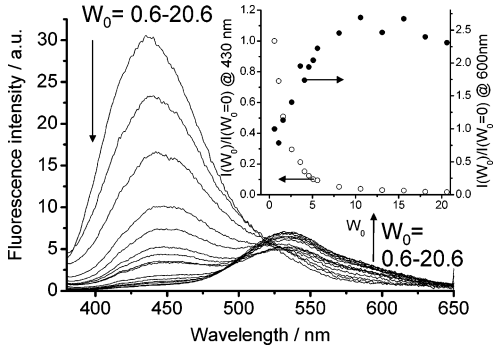

Figure 2. Fluorescence emission spectra of 7HQ in AOT/*n*-heptane reverse micelles with increasing W_0. Excitation wavelength: 371 nm. The spectra are corrected for the wavelength dependence of the detection and normalized for the absorption at the excitation wavelength. Inset: intensities at 430 and 600 nm divided by the respective intensities for $W_0 = 0.6$, as a function of W_0. The arrows indicate the trend of both bands as W_0 increases from 0.6 to 20.6.

2.2. Methods. UV−visible absorption and emission spectra were recorded on Varian (Cary E1) and Perkin-Elmer (LS-50B) spectrophotometers, respectively. Picosecond (ps) time-resolved emissions at magic-angle measurements were done by using a time-correlated single-photon-counting spectrophotometer (Fluo-Time 200) exciting at 371 or 433 nm (instrument response function (IRF) 65 ps operated at 10 MHz).[20] The decays were fitted by multiexponential functions convoluted with the IRF using the Fluofit package. Decay components down to 10 ps can be resolved after convolution, and this has been checked using short-lived (less than 10 ps decay time component) excited species and confirmed using femtosecond observation from this laboratory. The quality of the fits was characterized in terms of residual distribution, its autocorrelation, and the reduced χ^2 value. Time-resolved emission spectra (TRES) have been recorded from the decays measured at the different wavelengths of emission (32 decays) with a spectral interval of typically 6 nm. The spectra have been then constructed using the Fluofit package. The zero time has been defined at the channel corresponding to half of the maximum of the IRF at its rising part. The time-resolved area-normalized emission spectra (TRANES) have been constructed by area normalization of the TRES. All experiments were done at 293 ± 1 K.

3. Results and Discussion

3.1. Steady-State Observation. Figure 1 shows the absorption spectra of 7HQ in the reverse micelles upon increasing water concentration. In the absence of water, the spectrum is of the enol form (E).[21] The increase of water content (W_0 = 0.6 → 20.6) makes evident the appearance of the keto (K) or zwitterionic (Z) form (hereafter called tautomer, T, form) absorption at about 410 nm. $W_0 = 0.6$ corresponds to the sample without addition of water. At W_0 = 20.6, the absorption spectrum is still far from showing as much T absorption as in bulk water.[21,22] The new absorption band (410 nm) increases following a 1:2 stoichiometry complex formation, with an apparent equilibrium constant of 2 M^{-2} (inset in Figure 1). This process should involve the complexation of E with two water molecules to give an anion (A) which is converted to T.

The emission spectra of these samples upon excitation at 371 nm are shown in Figure 2. In the absence of added water the emission band (maximum intensity at 430 nm) does not correspond to any of the bands seen in pure water.[21] It is well-known that the E form emits at 380 nm, while the cation (C) and A emit at 450 and 490 nm, respectively.[21] For $W_0 < 5$ or in the absence of water within the AOT micelle, the dielectric constant of the pool is significantly lower than that of water,[5] and C cannot be produced with an anionic pool. This emission corresponds to an E form of 7HQ strongly bound (E···AOT) to the headgroups of AOT, with a strong anionic character.

TABLE 1: Values of Fluorescence Time Constants (τ_i) and Normalized Preexponential Factors (% A_i) at Three Emission Wavelengths (λ_{em}) and Increasing Water Content (W_0) of 7HQ/Water/AOT/*n*-Heptane

W_0	λ_{em}/nm	τ_1/ns	% A_1	τ_2/ns	% A_2	τ_3/ns	% A_3	χ^2
0.6	430	0.71	10			7.45[b]	90	1.397
	580	0.29	10			8.75[b]	90	1.030
1.1	430	0.60	16			7.01[b]	84	1.199
	505	0.04	(−)12			8.89[b]	88	1.098
1.6	430	0.21	14	1.68	27	6.20[b]	59	1.179
	505	0.01	(−)46	0.79	4	7.3[b]	50	1.079
	600			0.62	(−)21	7.15[b]	73	1.066
2.6	430	0.19	23	1.33	31	4.93[b]	46	1.132
	505	0.02	(−)51			5.45[b]	49	1.136
	600	0.06	(−)13	0.83	(−)28	3.62[b]	59	1.058
3.6	430	0.15	26	0.81	27	3.46	47	1.171
	505	0.01	(−)52	0.75	5	3.48	44	1.286
	600	0.06	(−)15	0.71	(−)26	3.6[b]	58	1.045
4.1	430	0.14	27	0.79	30	3.5[b]	44	1.140
	505	0.01	(−)50	0.50	6	3.00[b]	44	1.168
	600	0.04	(−)19	0.66	(−)25	3.46[b]	56	1.109
4.6	430	0.14	31	0.78	29	2.93	40	1.210
	505	0.01	(−)53	0.34	7	2.47	40	1.128
	600	0.03	(−)31	0.63	(−)21	2.90[b]	47	1.103
5.1	430	0.14	30	0.75	29	2.91	41	1.207
	505	0.01	(−)53	0.34	7	2.51	40	1.128
	600	0.05	(−)17	0.63	(−)25	3.07	59	1.077
5.6	430	0.12	34	0.66	28	2.46	38	1.125
	505	0.01	(−)56	0.28	10	2.13	35	1.195
	600	0.04	(−)18	0.61	(−)23	2.76	58	1.093
8.1	430	0.11	39	0.59	28	1.90	32	1.107
	505	0.01	(−)54	0.27	13	1.93	33	1.189
	600	0.03	(−)24	0.51	(−)20	2.73	57	1.20
10.6	430	0.11	40	0.52	27	1.65	33	1.107
	505	0.01	(−)51	0.27	14	1.96	34	1.138
	600	0.03	(−)24	0.50	(−)20	2.58	56	1.137
13.1	430	0.10	41	0.47	27	1.48	33	1.079
	505	0.01	(−)54	0.26	14	1.96	33	1.125
	600	0.03	(−)25	0.51	(−)18	2.58	57	1.277
15.6	430	0.10	41	0.43	25	1.35	34	1.041
	505	0.01	(−)51	0.27	14	2.07	35	1.158
	600	0.03	(−)24	0.52	(−)17	2.55	58	1.170
18.1	430	0.08	39	0.36	27	1.27	34	1.049
	505	0.01	(−)58	0.28	12	2.09	30	1.096
	600	0.04	(−)20	0.50	(−)18	2.54	62	1.205
20.6	430	0.06	36	0.30	29	1.19	35	1.123
	505	0.01	(−)52	0.29	13	2.16	35	1.167
	600	0.04	(−)19	0.50	(−)18	2.57	63	1.335

[a] (−), negative amplitude, percentage calculated with absolute values. [b] The fixed parameter during fitting, obtained at longer time scales.

However, we cannot exclude the very few molecules of water (0.15%) that are attached to these heads and that might be involved in the formation of this blue emitting species. Indeed these molecules are necessary to stabilize the transferred proton to the AOT heads. The emission (430 nm) resembles the A band in R2PI (resonant two photon ionization) supersonic-jet experiments with 7HQ·$(NH_3)_n$ clusters (444 nm).[23] Note that the excitation at 330 nm gives emission bands at 380 and 530 nm according to a previous work.[18] As the water content increases, the emission at 430 nm is quenched and slightly shifts up to 10 nm to the red.

Clearly, at small water content, $W_0 \approx 2$, another emission band appears at 530 nm and its intensity continues to increase until saturation at $W_0 \approx 10$. Based on previous reports, we assign this band to the emission of the T form.[21,23] It does not suffer any shift. The fact that the quenching efficiency of the bound E form emission grows monotonically (inset in Figure 2) and the emission of T saturates indicates that T photoformation comes from both excited-state reaction of E···AOT and direct excitation of T populated at the ground state.

3.2. Time-Resolved Observation. Upon excitation at 371 nm, compared to the observation at larger W_0 values, the fluorescence decay of 7HQ within the micelle at $W_0 = 0.6$ shows a small variation with the emission wavelength. Though the emission is not monoexponential (0.71 and 7.45 ns at 430 nm, and 0.29 and 8.75 ns at 580 nm; Table 1), only one band can be recorded in the time-resolved spectrum, shown in Figure 3. The band is attributable to the E strongly bound to the heads of AOT as explained above. Within the picosecond regime, the constructed solvation dynamics correlation function, $C(t)$, shows a biexponential decay with time constants of 20 ps (13%) and 1.81 ns (87%) (inset in Figure 3). Because in nonpolar and non-H-bonding solvents the emission is due to E (380 nm), it is not possible to use, as has been done in other systems,[24] the related spectra to extract the zero-time emission spectrum of the E form bound to the AOT headgroups. The involved species of 7HQ in an apolar medium and in the AOT system are completely different. Therefore, zero time was defined as explained in section 2.2, Methods. The extracted times are different from those of the previously reported $C(t)$ for coumarin 152 in the same environment,[25] where a ~15 ns component was explained in terms of ionic motion inside the pool. Although the mean emission lifetime observed for 7HQ (7.45 ns) in the reverse micelle is much longer than that observed for the coumarin (4 ns), we could not detect the 15 ns component in $C(t)$ decay. This difference could reflect either a different degree of

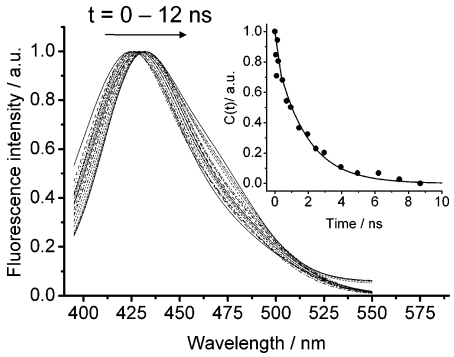

Figure 3. Time-resolved emission spectra of 7HQ in AOT/*n*-heptane reverse micelles at $W_0 = 0.6$. Excitation wavelength: 371 nm. The fluorescence maximum energies at $t \approx 0$ and ∞ and total dynamic Stokes shift are, respectively, $\bar{\nu}_0 = 23\,534$ cm^{-1}, $\bar{\nu}_\infty = 23\,004$ cm^{-1}, and $\Delta\bar{\nu}_{0-\infty} = 530$ cm^{-1}. The inset shows the corresponding solvation correlation function, $C(t)$, fitted (time constants in nanoseconds) with $C(t) = 0.13\exp(-t/0.02) + 0.87\exp(-t/1.81)$.

attachment of these probes to the micellar headgroups or a different localization inside the micelle (trapped between the alkyl chains—unlikely for 7HQ—or inside the "pool").

When we increased the water content, several features of the decay noticeably changed: a rise was observable at long wavelengths as the A and the T forms appeared, and all processes accelerated. Figure 4 shows the emission signal for $W_0 = 20.6$ and at different wavelengths of observation. The figure also shows how the short components, decaying at 430 nm, and rising at 600 nm, evolve with W_0. To begin with a simple and interesting observation, two main behaviors can be inferred following the value of W_0. Below $W_0 \approx 5$, the time constants change dramatically (100% at 430 nm), and above this limit there is no or weak variation. The value of $W_0 \approx 5$ corresponds to the amount of water argued to be needed to start having "free" water molecules inside the nanopool.[26] Terahertz spectroscopic measurements have found that the nanopool for W_0 below 3 is substantially different from that above this value. The collective relaxation modes of water are suppressed by the confinement when the nanopool of free water has a radius smaller than 8 Å.[13] Furthermore, at a W_0 value of 5 the viscosity of the water nanopool reaches a plateau (<30 cP), as measured by means of fluorescence quantum yield variation of auramine-O.[27] Data of picosecond time-resolved anisotropy ($r(t)$) measurements agree with this result and strength our argument. Using the wobbling-in-cone analysis of $r(t)$ decays when increasing W_0, around $W_0 = 5$ the result shows two different regimes of lateral diffusion relaxation time. The work will be soon submitted for publication.[28]

Both short (Figure 4B) and long (Figure 4C) decay components at 430 nm suffer about a 10-fold decrease when W_0 is increased (from 710 to 60 ps and from 1.68 to 0.30 ns, respectively), while for the rising components at 600 nm only a lower change is observed (from 60 to 40 ps and from 830 to 500 ps, respectively; see also Table 1). These differences are rather complex to be explained quantitatively because the excitation (371 nm) is placed at a wavelength of absorption of all three involved and water bound species: E, A, and T. It is not possible to establish their relative contributions and absolute emission quantum yields. Nevertheless, some of the decay components can be assigned to different reaction steps, especially the rising components observed at 600 nm, as depicted in Figure 5. Both times (~50 ps, 500−830 ps) reflect the formation of T from A. The short one comes from a directly excited A, while the longer one is from A produced after a single

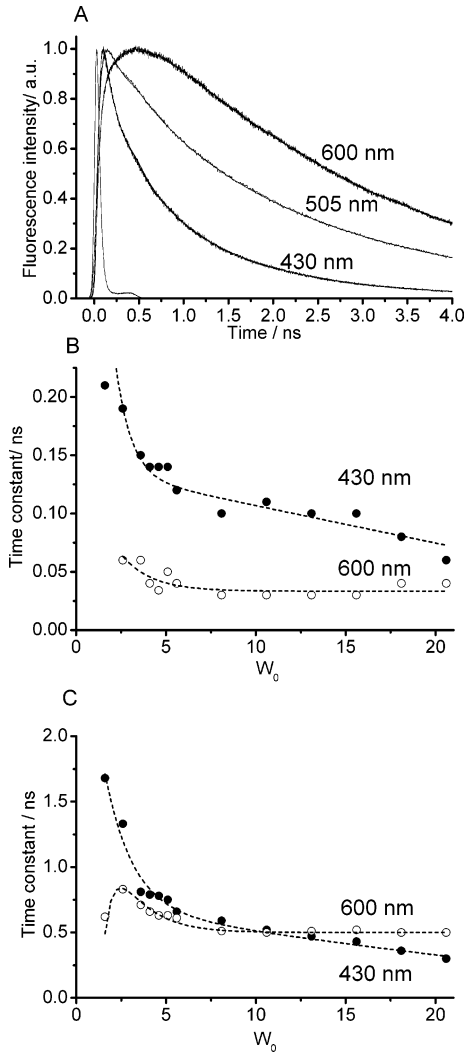

Figure 4. (A) Fluorescence decays of 7HQ in AOT/*n*-heptane reverse micelles at 430, 505, and 600 nm at $W_0 = 20.6$. (B, C) Variation of time constant values for shortest components at 430 (filled circles) and 600 nm (empty circles) decays. All components at 430 nm have positive amplitudes, and those at 600 nm have negative ones. The spline lines are drawn just to guide the eye. Excitation wavelength: 371 nm.

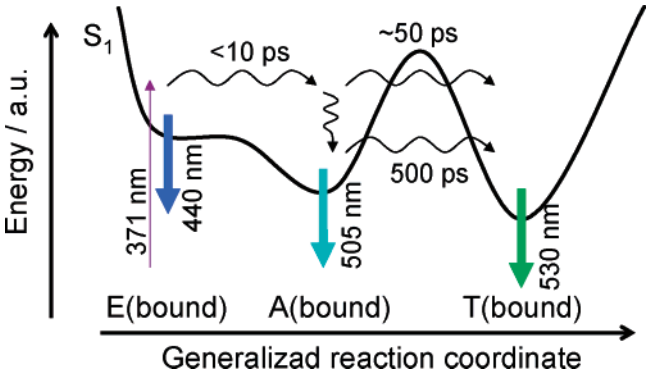

Figure 5. Simplified potential-energy surface of the electronically first excited-state proton-transfer reactions experienced by 7HQ in water/AOT/*n*-heptane reverse micelles upon excitation at 371 nm. The given values are for $W_0 = 20.6$, and the energy barriers are not to scale. See text for details.

proton-transfer reaction in bound E. The difference in time is due to the slowest solvent reorganization in the latter mechanism. Any reaction of bound E form involves a large solvent reorganization due to the water molecules attached to the AOT

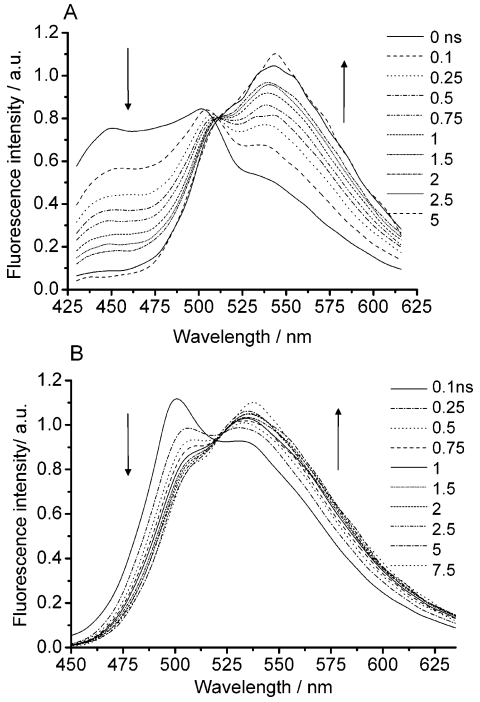

Figure 6. Time-resolved area-normalized emission spectra of 7HQ in AOT/*n*-heptane reverse micelles at $W_0 = 20.6$ upon excitation at 371 (A) and 433 nm (B). The insets give the corresponding gating times.

heads. This assignment is confirmed by the results obtained when exciting at a longer wavelength (433 nm) and in deuterated water (vide infra). The 430 nm emission decay components are due to the emissions of bound E to give bound A, and of A to give T.

To get spectral information on the dynamics, the time-resolved emission spectra (Figure 6) in the TRANES representation[29] have been recorded. These spectra show a peak at about 505 nm present in all water concentrations above $W_0 \approx 2$, but not visible in the steady-state spectra. We suggest that it originates from A, but it is only apparent under high repetition (10 MHz, 100 ns between two pulses) and moderately high pump energy (about 0.4 mW) of the 371 nm diode laser used in the picosecond experiment. A likely explanation is that the ground-state equilibrium between A and the other forms (E and T) is not reestablished from one pulse to the next one, leading to an A ground-state concentration larger than that in the steady-state fluorescence conditions. According to a microsecond-resolved study of 7HQ in water, the ground-state reaction from T to E proceeds within 20 μs.[8] Hence, within this time (20 μs), 200 pulses, separated by 0.1 μs, have been delivered to the sample increasing then the population of A and T at S_0 after relaxation from S_1, and they will accumulate during their ground-state lifetimes. The above proposed explanation for the enhanced A emission is coherent with the experimental findings if a nondetected intermediate step to A is also comparably slow in the ground state.

The 505 nm emission band is linked by an isoemissive point to the T emission but not to the E-bound one (Figure 6A). Therefore, and because the rising component at 505 nm is shorter than 10 ps and insensitive to the water content, the A structure has to be formed in a short time, or by direct excitation of its population at S_0. At S_1, A reaction leads to T by proton transfer from water molecules to the pyridinic nitrogen. The fact that the photoreaction of A at $W_0 = 20.6$ occurs in 290 ps, a time shorter than the rise of T (500 ps, at the same water concentration), might be due to the strong overlap between the

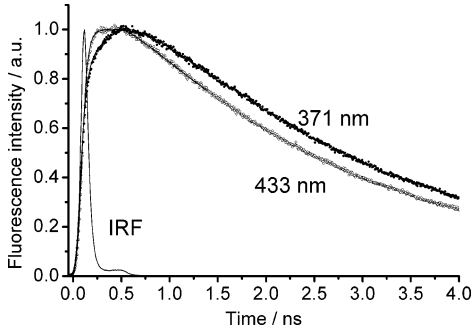

Figure 7. Fluorescence decays of 7HQ in AOT/*n*-heptane reverse micelles at $W_0 = 20.6$ recorded at 600 nm, upon excitation at 371 and 433 nm.

emissions of A and T at the interrogated wavelength for A. In this region we have the decay and rise of a similar time constant, and it is not easy to extract the corresponding value. To get more information on A and T population dynamics, we excited in their absorption regions, and studied the isotope effect (H_2O/D_2O exchange).

3.3. Excitation Wavelength and Isotopic Effects. Excitation at 433 nm and detection at 600 nm in $W_0 = 20.6$ micelles (Figures 6B and 7) yield a decay comparable to that observed upon excitation at 371 nm with some differences in the rising components: the 500 ps one becomes shorter, 340 ps, and its contribution smaller, from 18 to 7% (Table 2). The shortest rise diminishes from 40 to 20 ps, but its contribution doubles from 19 to 38%. The decay time value of T stays at 2.5 ns, and its contribution goes from 63 to 55%. The decrease in both components when we shift the excitation to the red side of the absorption spectrum is due to the higher proportion of directly excited T form (Figure 2). The fact that both components are measurable confirms the proposed mechanism (Figure 5): both short and long rising components are due to the production of T from A. Furthermore, at 433 nm excitation, the TRANES shows only the 505 and the 530 nm bands. In the time-integrated spectra (not shown) obtained from the TRANES, the T band has a relatively higher intensity with 433 nm excitation than with 371 nm. In ref 18, no rising component was found upon 435 nm excitation, and there is no mention of the presence of the 505 nm band. We have no explanation for this disagreement except for a possible different sensitivity of the used picosecond systems.

From the above results it is clear that the potential-energy surface (PES) at S_1 has a significant energy barrier in the second step involving A photoreaction to produce T. Therefore, to get information on the nature of reaction dynamics of E···H_2O and A···H_2O, we studied the isotope effect on the water nanopool dynamics. We performed picosecond emission measurements using D_2O at $W_0 = 5.6$ and 20.6 (Figure 8). It is remarkable that although there is no effect on the decay of bound E (430 nm), the isotope effect is rather significant for A (505 nm) and T (600 nm). The related data are shown in Table 3. Both the rise and decay of T are about 2 times slower than in the H_2O nanopool on either W_0 (for 600 nm at $W_0 = 20.6$, the decays in water give 40 ps (−19%), 500 ps (−18%), 2.57 ns (63%); and in D_2O give 70 ps (−22%), 660 ps (−15%), 5.91 ns (63%)).

We begin with the difference in the nanosecond components in both media, attributable to the lifetime of T, and explain it by the following. It is known that a close low lying triplet state of T is present, and an intersystem crossing time constant of 3 ns has been measured in water.[8] In D_2O, the rate of intersystem crossing could be affected, increasing the S_1 lifetime, since the interstate overlap might be reduced under deuteration.[30] Another

TABLE 2: Values of Fluorescence Time Constants (τ_i) and Normalized Preexponential Factors (% A_i) at Different Excitation (λ_{ex}) and Emission (λ_{em}) Wavelengths of 7HQ/Water/AOT/*n*-Heptane ($W_0 = 20.6$)

λ_{em}/nm	λ_{ex}/nm	τ_1/ns	% A_1	τ_2/ns	% A_2	τ_3/ns	% A_3	χ^2
505	371	0.01	(−)52	0.29	13	2.16	35	1.167
	433	0.13	19	0.53	24	2.39[b]	57	1.102
600	371	0.04	(−)19	0.50	(−)18	2.57	63	1.335
	433	0.02	(−)38	0.34	(−)7	2.50[b]	55	0.998

[a] (−), negative amplitude, percentage calculated with absolute values. [b] The fixed parameter during fitting, obtained at longer time scales.

TABLE 3: Values of Fluorescence Time Constants (τ_i) and Normalized Preexponential Factors (% A_i) at Two Emission Wavelengths (λ_{em}) of 7HQ in Water/AOT/*n*-Heptane at $W_0 = 5.6$ and $W_0 = 20.6$ for H_2O and D_2O

W_0	λ_{em}/nm	pool solvent	τ_1/ns	% A_1	τ_2/ns	% A_2	τ_3/ns	% A_3	χ^2
5.6	505	H_2O	0.01	(−)56	0.28	10	2.13	35	1.195
		D_2O	0.50	21	1.88	27	5.58	52	1.115
	600	H_2O	0.04	(−)18	0.61	(−)23	2.76	58	1.093
		D_2O			0.98	(−)34	6.23	66	1.206
20.6	505	H_2O	0.01	(−)52	0.29	13	2.16	35	1.167
		D_2O	0.45	26	1.50	14	5.70	60	1.095
	600	H_2O	0.04	(−)19	0.50	(−)18	2.57	63	1.335
		D_2O	0.07	(−)22	0.66	(−)15	5.91	63	1.221

[a] (−), negative amplitude, percentage calculated with absolute values.

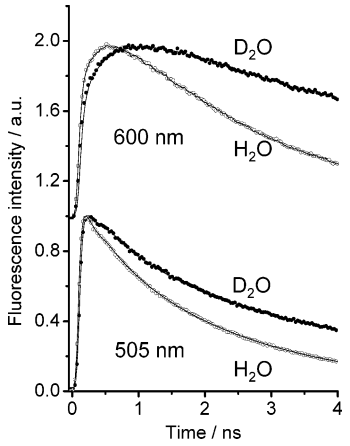

Figure 8. Fluorescence decays of 7HQ in AOT/*n*-heptane reverse micelles containing H_2O or D_2O ($W_0 = 20.6$) recorded at 505 and 600 nm, and upon excitation at 371 nm.

explanation, already pointed out for 7HQ and 7-azaindole (7AI), is based on the reduction of the nonradiative rates of T.[22d,31] The internal conversion to the ground state is thought to be governed by a coupling of N−H stretching and the ring vibrations, altered by the NH/ND exchange. The role in the energy release ability of the NH/ND stretching mode has been invoked to explain the kinetic isotope effect (KIE) in the internal conversion of rhodamines.[32] Therefore the NH/ND vibration influences the internal conversion process, leading to an increase of the emission lifetime as observed here.

A few years ago, we showed that 7HQ forms two different complexes with water. We have shown that a 1:2 (7HQ:H_2O) complex in a molecular beam is not able to exhibit any proton-transfer reaction,[33] as recently confirmed by others.[34] For α-naphthol it has been shown that a minimum of accepting solvent molecules is necessary to take and solvate the proton.[35] For 7HQ in water, the structure of the complexes depends on the O−H conformation of the dye, and the kind of stoichiometry.[33,34] For a double-proton-transfer reaction the cis complexed conformer will need more time to react than the trans one to form the T tautomer. The coexistence of both cis and trans conformers in the micelle will then give a more complex kinetics, for both H_2O and D_2O nanopools. Furthermore, the population of bound A and T must change at S_0 as the proton (deuteron) reactions to generate them have energy barriers and might occur through tunneling. The equilibrium constants at S_0 might be affected in different ways.

The lack of KIE in the 430 nm decay is coherent with the missing isoemissive point between the 430 and the 505 nm bands in the TRANES (Figure 6A). The reaction step producing A from the bound E form is in the limit of, or faster than, the time resolution of the apparatus. Furthermore, no rise can be clearly measured at 505 nm (vide supra). Femtosecond experiments from this laboratory[36] have shown that within the micelle the A structure is formed in a time shorter than 1 ps. Thus, being a barrierless process, no KIE is expected for the formation of A. In contrast, the formation of T is sensitive to the H_2O/D_2O exchange and the fast decay component of A shows the associated change. The extent of KIE ($k(H_2O)/k(D_2O)$) is about 1.8 and 1.3 for the short and long rising components at 600 nm, respectively. These values are close to the square root of the D/H mass ratio, as expected. Application of the unidimensional tunneling model[37] for the nitrogen protonation of A leads to a rate constant several orders of magnitude faster in water than in a deuterated solvent. This result means that any channel producing T is controlled not only by the elementary H-transfer step, but also by the solvent reorganization involving the breaking and making of H(D)-bonds in the network within the micelle. Previously, a KIE above 2, and independent of W_0 in the 4−32 range, has been reported.[18] However, this result cannot be directly compared to ours due to the difference in the excitation wavelength (315 nm in ref 18). Nevertheless, it is noticeable that their observed KIE for the rising component at long wavelengths of emission is about 1.8, as we have measured exciting at 371 nm. Their results were explained arguing that 7HQ is located in the bound-water region and not in the free-water region. Moreover, they considered the solvent reorganization to be the rate-determining factor of the reaction, hence the relatively low KIE.

Our results show that when the amount of water in the nanopool is small ($W_0 < 5$) the structural changes due to the translational and rotational motion of the few "biological " water molecules are so slow that the photoreaction of A (formed from bound E) occurs in ∼600 ps. At $W_0 \geq 5$ the change becomes faster, probably involving "free" water molecules, and therefore leading to a shorter reaction of the H-bond network. At $W_0 = 20.6$, the time for A reaction is 290 ps. In the absence of water or at very low W_0 values, 7HQ is near the "dry" AOT

headgroups, giving a slow response. Upon increasing W_0, the AOT heads become hydrated, and the distribution of the probe becomes heterogeneous; some 7HQ molecules might be located in the water nanopool (femtosecond to picosecond response) and others still near the micelle heads. Thus, the slow contribution of AOT heads in the solvation dynamics becomes lower when the content of water within the micelle increases and that of the faster water molecules becomes dominant. Figure 5 displays a proposed PES at S_1. Direct excitation of A leads to T in ~50 ps. However, a similar reaction takes place in 500−830 ps when A is formed from E···H_2O. As stated above, the difference in time is due to the evolution of the system in the latter case through a reaction coordinate involving a larger structural change of the surrounding solvation shell in the nanopool. Scheme 1 displays a representation of 7HQ within the AOT/*n*-heptane micelle system, and for a situation where most of the probe is in the water pool corresponding to a large W_0.

4. Conclusion

This work reports on picosecond dynamics of water within a micelle nanopool. It gives clues about the behavior of water molecules inside the micelle. Two distinct regimes of the pool are observed from the kinetics: a regime below $W_0 \approx 5$ (300 water molecules) having slow dynamics, and a much faster regime above this limit. This means that at about 300 water molecules inside the micelle the transition between both regimes can be observed, and above it the behavior of the network does not significantly change. It is important, nevertheless, to point out that, even at the higher water concentration studied, the kinetics are never as fast as in pure water. Reverse micelles containing up to several thousand water molecules still "feel" the nanopool confinement effect. Note also that a probe distribution between the free (faster into the pool) and bound (slower near the headgroups of AOT) water regions should contribute to the observed changes in the picosecond dynamics. Finally, 7HQ in the micelle gives four species at S_1: free and bound enol, anion, and tautomer structures, having emission maxima at 380, 430, 505, and 530 nm, respectively.

Acknowledgment. This work was supported by MEC and JCCM (Consejerías de Sanidad y de Educación y Ciencia) through Projects CTQ2005-00114, SAN-04-000-00, and PBI-05-046.

References and Notes

(1) Pal, S. K.; Zewail, A. H. *Chem. Rev.* **2004**, *104*, 2099.

(2) Nandi, N.; Bhattacharyya, K.; Bagchi, B. *Chem. Rev.* **2000**, *100*, 2013. Bhattacharyya, K. *Acc. Chem. Res.* **2003**, *36*, 95. Bhattacharyya, K.; Bagchi, B. *J. Phys. Chem. A* **2000**, *104*, 10603.

(3) Chang, G.-G.; Huang, T.-M.; Hung, H.-C. *Proc. Natl. Sci. Counc., Repub. China, Part B* **2000**, *24*, 89.

(4) See, for example: Levinger, E. *Science* **2002**, *298*, 1722 and references therein.

(5) Cohen, B.; Huppert, D.; Solntsev, K. M.; Tsfadia, Y.; Nachliel, E.; Gutman, M. *J. Am. Chem. Soc.* **2002**, *124*, 7539.

(6) Klymchenko, A. S.; Demchenko, A. P. *Langmuir* **2002**, *18*, 5637.

(7) Kwon, O.-H.; Jang, D.-J. *J. Phys. Chem. B* **2005**, *109*, 20479.

(8) Lee, S.-I.; Jang, D.-J. *J. Phys. Chem.* **1995**, *99*, 7537.

(9) García-Ochoa, I.; Bisht, P. B.; Sánchez, F.; Martinez-Atáz, E.; Santos, L.; Tripathi, H. B.; Douhal, A. *J. Phys. Chem. A* **1998**, *102*, 8871.

(10) García-Ochoa, I.; Díez López, M.-A.; Viñas, M. H.; Santos, L.; Martinez-Atáz, E.; Sánchez, F.; Douhal, A. *Chem. Phys. Lett.* **1998**, *296*, 335.

(11) Kwon, O.-H.; Lee, Y.-S.; Yoo, B. K.; Jang, D.-J. *Angew. Chem., Int. Ed.* **2006**, *45*, 415.

(12) Piletic, I. R.; Tan, H.-S.; Fayer, M. D. *J. Phys. Chem. B* **2005**, *109*, 21273. Tan, H.-S.; Piletic, I. R.; Fayer, M. D. *J. Chem. Phys.* **2005**, *122*, 174501.

(13) Mittelman, D. M.; Nuss, M. C.; Colvin, V. L. *Chem. Phys. Lett.* **1997**, *275*, 332.

(14) Solber, J. J.; Biasutti, A.; Abui, E.; Lissi, E. *Adv. Colloid Interface Sci.* **1999**, *82*, 189.

(15) De T. K.; Maitra, A. *Adv. Colloid Interface Sci.* **1995**, *59*, 95.

(16) See, for example: Hazra, P.; Chakrabarty, D.; Sarkar, N. *Langmuir* **2002**, *18*, 7872. Hazra, P.; Chakrabarty, D.; Sarkar, N. *Chem. Phys. Lett.* **2003**, *371*, 553.

(17) See, for example: Wittouck, N.; Negri, B. M.; Ameloot, M.; de Schryver, F. C. *J. Am. Chem. Soc.* **1994**, *116*, 10601.

(18) Kwon, O.-H.; Kim, T. G.; Lee, Y.-S.; Jang, D.-J. *J. Phys. Chem. B* **2006**, *110*, 11997.

(19) Zulauf, M.; Eicke, H.-F. *J. Phys. Chem.* **1979**, *83*, 480. Riter, R. E.; Willard, D. M.; Levinger, N. E. *J. Phys. Chem. B* **1998**, *102*, 2705.

(20) Organero, J.-A.; Tormo, L.; Douhal, A. *Chem. Phys. Lett.* **2002**, *363*, 409.

(21) Mason, S. F.; Philp, J.; Smith, B. E. *J. Chem. Soc., A* **1968**, *12*, 3051.

(22) (a) Itoh, M.; Adachi, T.; Tokomura, K. *J. Am. Chem. Soc.* **1983**, *105*, 4828. (b) Bardez, E.; Fedorov, A.; Berberan-Santos, M. N.; Martinho, J. M. G. *J. Phys. Chem. A* **1999**, *103*, 4131. (c) Kim, T. G.; Topp, M. R. *J. Phys. Chem. A* **2004**, *108*, 10060. (d) Park, H. J.; Kwon, O.-H.; Ah, C. S.; Jang, D.-J. *J. Phys. Chem. B* **2005**, *109*, 3938.

(23) Bach, A.; Leutwyler, S. *J. Chem. Phys.* **2000**, *112*, 560.

(24) Fee, R. S.; Maroncelli, M. *Chem. Phys.* **1994**, *183*, 235.

(25) Hazra, P.; Chakrabarty, D.; Sarkar, N. *Langmuir* **2002**, *18*, 7872.

(26) D'Aprano, A.; Lizzio, A.; Turco Liveri, V.; Aliotta, F.; Migliardo, P. *J. Phys. Chem.* **1988**, *92*, 4436.

(27) Hasegawa, M.; Sugimura, T.; Shindo, Y.; Kitahara, A. *Colloids Surf. A* **1996**, *109*, 305.

(28) Douhal, A.; et al. To be submitted for publication.

(29) Laguitton-Pasquier, H.; Pansu, R.; Chauvet, J.-P.; Pernot, P.; Collet, A.; Faure, J. *Langmuir* **1997**, *13*, 1907. Koti, A. S. E.; Krishna, M. M. G.; Periasamy, N. *J. Phys. Chem. A* **2001**, *105*, 1767.

(30) Amirav, A.; Sonnenschein, M.; Jortner, J. *Chem. Phys. Lett.* **1983**, *100*, 488.

(31) Chou, P.-T.; Yu, W.-S.; Wei, C.-Y.; Cheng, Y.-M.; Yang, C.-Y. *J. Am. Chem. Soc.* **2001**, *123*, 3599.

(32) Ferreira, J. A. B.; Costa, S. M. B. *Chem. Phys.* **2006**, *321*, 197.

(33) Lahmani, F.; Douhal, A.; Breheret, E.; Zehnacker-Rentien, A. *Chem. Phys. Lett.* **1994**, *220*, 235.

(34) Tanner, C.; Thut, M.; Steinlin, A.; Manca, C.; Leutwyler, S. *J. Phys. Chem. A* **2006**, *110*, 1758. Matsumoto, Y.; Ebata, T.; Mikami, N. *Chem. Phys. Lett.* **2001**, *338*, 52.

(35) Kim, S. K.; Breen, J. J.; Willberg, D. M.; Peng, L. W.; Heikal, A.; Syage, J. A.; Zewail, A. H. *J. Phys. Chem.* **1995**, *99*, 7421. Kim, S. K.; Wang, J.-K.; Zewail, A. H. *Chem. Phys. Lett.* **1994**, *228*, 369.

(36) Douhal, A.; et al. Presented at the Femtochemistry VI Conference, Paris, 2003.

(37) Hineman, M. F.; Brucker, G. A.; Kelley, D. F.; Bernstein, E. R. *J. Chem. Phys.* **1992**, *97*, 3341.